Mechanical Analysis and Numerical Simulation for New Type of Dynamic Control Devices

CHEN Suhua[1,2*], LI Ruiqi[2], FEI Liang[2], YU Zhiguang[2], DING Jianming[1,2]

1. School of Transportation, Southeast University, Nanjing 210096, P.R. China;
2. Architects & Engineers Co., Ltd., Southeast University, Nanjing 210096, P.R. China

Abstract: The conventional dynamic control devices, such as fluid viscous damper (VFD) and isolating bearings, are unsuitable for the double-deck cable-stayed bridge due to a lack of sustainability, so it is necessary to introduce some high-tech dynamic control devices to reduce dynamic response for double-deck cable-stayed bridges under earthquakes. A (90+128) m-span double-deck cable-stayed bridge with a steel truss beam is taken as the prototype bridge. A 3D finite element model is built to conduct the nonlinear time-history analysis of different site categories in fortification intensity Ⅸ (0.40 g) degree area. Two new types of dynamic control devices-cable sliding friction aseismic bearings (CSFABs) and elasticity fluid viscous dampers composite devices (EVFDs) are introduced to reduce the dynamic responses of double-deck cable-stayed bridges with steel truss beam. The parametric optimization design for the damping coefficient C and the elastic stiffness of spring K of EVFDs is conducted. The following conclusions are drawn: (1) The hybrid support system by EVFDs and CSFABs play a good function under both seismic and regular work, especially in eliminating the expansion joints damage; (2) The hybrid support system can reduce the beam-end displacement by 75% and the tower-bottom bending moment by 60% under the longitudinal seismic excitation. In addition, it can reduce the pier-bottom bending moment by at least 45% under transverse seismic and control the relative displacement between the pier and beam within 0.3 m. (3) Assuming the velocity index $\alpha=0.3$, the parametric optimization suggests the damping coefficient C as 2 000 kN·s·m^{-1} in site Ⅰ0, 4 000 kN·s·m^{-1} in site Ⅱ, 6 000 kN·s·m^{-1} in site Ⅳ, and the elastic stiffness of spring K as 10 000 kN/m in site Ⅰ0, 50 000 kN/m in site Ⅱ, and 100 000 kN/m in site Ⅳ.

Key words: dynamic control device; double-deck cable-stayed bridge with steel truss beam; cable-sliding friction aseismic bearings (CSFABs); elasticity fluid viscous dampers composite devices (EVFDs)

CLC number: TU318   **Document code:** A   **Article ID:** 1005-1120(2022)06-0735-15

0 Introduction

Double-deck cable-stayed bridges with steel truss beams is a new type of highway bridges that can solve the problem of increasing traffic and limited supply of land. In the past, the cable-stayed bridge with steel truss beams was widely used in railway bridges. In recent years, the growth of traffic and the development of urban expressways demand bridges to be open both at the upper and the lower decks. Further, the double-deck cable-stayed bridges with steel truss beams have a rapid development because of their large range of spans[1].

Double-deck cable-stayed bridges with steel truss beams carry heavier traffic than single-deck cable-stayed bridges. However, steel truss beams cause an increase in dead load, leading to increased substructure dynamic responses and superstructure seismic displacements. Besides, steel truss beams with higher lateral stiffness cause an increase in transverse seismic responses, which leads to high bearing shear force and a possibility of beam dropping under an earthquake. Double-deck bridges have

a higher risk of lateral sliding with beam-dropping than single-deck bridges because of the high truss, which maybe causes unforeseeable damages. Therefore, it is necessary to adopt the dynamic control devices[2-4] to reduce seismic responses for double-deck cable-stayed bridges with steel truss, both in longitudinal and transverse directions.

At present, the fluid viscous damper (VFD) is one of the most important dynamic control devices for bridges and has been widely used in the engineering field worldwide[5-7]. However, it has been proved that the conventional VFD may cause damages to beam-end expansion joints for various live loads in service, including temperature, vehicles, and wind[8]. In particular, dampers cannot pull the main beam back to the original positions, and the cumulative deformation may exceed the allowable design value of expansion joints and support bearings. Double-deck bridges are open to traffic at both the upper and the lower decks, so they have a higher requirement for the performance and sustainability of the expansion joints to avoid water leakage and deformation damage of joints. It is necessary to consider the performance of expansion joints in the seismic reduction and isolation design for double-deck cable-stayed bridges with steel truss beam.

There are several studies on the seismic reduction of the double-deck cable-stayed bridges. Jiao Changke from Southeast University[9] conducted a research on the effect of wave excitation and random response on double-deck cable-stayed bridges. Xing Liang[10] analyzed the natural vibration mode and seismic response of double-deck cable-stayed bridges. Zhang Yu[11] conducted an analysis of the seismic response of different structural systems of steel truss cable-stayed bridges. However, most of them adopted the conventional dampers for longitudinal seismic isolation design. The sustainability of expansion joints are neglected. In addition, the research on transverse seismic isolation design of the double-deck cable-stayed bridge is still on demand, and the influence of site types on the seismic responses is also insufficient. Transverse seismic isolation design of the double-deck cable-stayed bridge and the influence of site types on the dynamic responses should

be further investigated.

This paper puts forward a new composite system of dynamic control devices with the cable-sliding friction aseismic bearings (CSFABs) and the elasticity fluid viscous dampers composite devices (EVFDs). It can solve the problem of transverse seismic isolation design and improve the sustainability of the expansion joints.

1 New Types of Dynamic Control Devices

In recent years, many conventional dynamic control devices have been improved to adapt to the different structure and functional demands, including CSFABs[12-13] and EVFDs[8]. The two devices have one thing in common: They both adopt elastic elements to improve seismic-reduction performance and sustainability in the operation stage.

1.1 CSFABs

CSFABs comprise general spherical steel bearings and elastic cables. Fig.1 shows the composition of CSFABs. This seismic isolation device is suitable for bridges with large shear forces of bearings under ground motions. It can reduce dynamic responses by releasing the constraints between superstructure and substructure to limit the displacement of deck systems to an allowed range. It has been used in some cable-stayed bridges to solve the bearing damages on side piers under transverse excitation[14-16]. After the transverse shear of the support bearings, there will be a relative displacement between the pier and the beam. When the relative displacement reaches a specific value called free-displacement (u_0), the cables will tie up the beam, as shown in Fig.2. This scheme can obviously reduce

Fig.1　Composition of CSFABs

(a) Normal working condition

(b) Earthquake condition
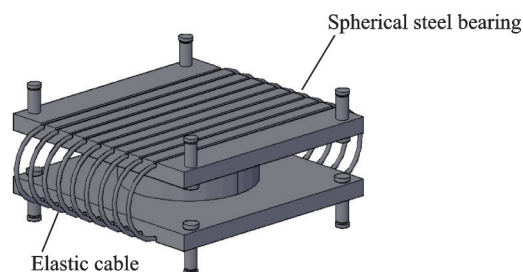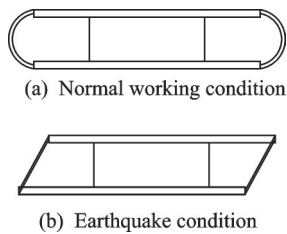
Fig.2　Operating mode of CSFABs

the side pier internal force and have a reasonable displacement restriction for truss beams to avoid beam falling.

The constitutive law of CSFABs can be considered as a combination of sliding spherical steel bearings and elastic cables. The constitutive law of the sliding spherical steel bearing is similar to that of ideal elastic-plastic materials, and the constitutive law of the elastic cable is a linear model.

As shown in Fig.3, k_1 is the elastic stiffness of sliding bearings, f_y the critical friction force of bearing, k_2 the horizontal stiffness of the cable, and u_0 the free displacement. When the relative displacement is below u_0, it works like general sliding bearings. When the relative displacement is upper u_0, elastic cables begin to work.

(a) Sliding spherical bearing　(b) Elastic cable　(c) CSFABs
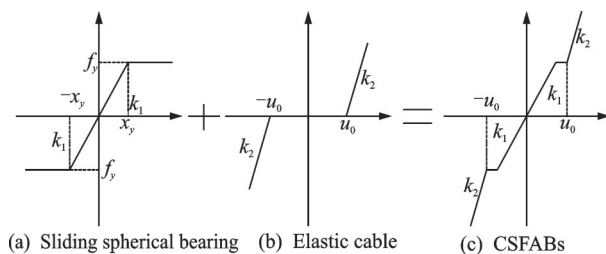
Fig.3　Constitutive law of CSFABs

Generally, the critical friction force f_y and the elastic stiffness of sliding bearing k_1 can be expressed as

$$f_y = \mu R = k_1 x_y \tag{1}$$

where μ is the sliding friction coefficient that usually adopts 0.02; R the gravity of superstructure borne by bearings; and x_y the relative displacement between the pier and the beam. In sliding spherical steel bearings, a relative displacement is realized almost entirely via the relative sliding between a Polytetrafluoroethene (PTFE) sliding plate and a stainless steel plate. Hence, x_y is very small and can

be set as 2 mm.

1. 2　EVFDs

EVFDs can be divided into two parts, VFDs and the elastic spring[8]. Fig.4 shows the composition of EVFDs. The composite device houses an elastic spring outside the cylinder of conventional dampers. The elastic part works independently from the damper part. The dampers provide damping forces, and the elastic spring provides restoring forces. Generally, the VFDs mainly provide damping under earthquakes and have a much lower effect under the normal working state. But the elastic spring mainly provides elastic stiffness under earthquakes and the normal working state. The composite device can reduce the displacements and dynamic wear of expansion joints, therefore keep itself durably. EVFDs have been used in long-span cable-stayed bridges to reduce longitudinal seismic responses and ensure the expansion joints normally working.
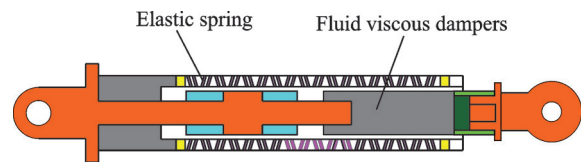
Fig.4　Composition of EVFDs

The constitutive law of the EVFDs can be expressed as

$$F = KX + CV^\alpha \tag{2}$$

where C is the damping coefficient; V the relative velocity between the two connection ends; α the velocity index; K the elastic spring stiffness; and X the relative displacement between the two connection ends.

1. 3　Composite system of CSFABs and EVFDs

CSFABs is usually used in transverse seismic isolation design, while EVFDs is usually used in longitudinal seismic isolation design. So it can be inferred that a reasonable combination of the two dynamic control devices will work under the earthquake in all directions.

A double-deck cable-stayed bridge with a steel truss beam is taken as an example to carry out the

research on the longitudinal and transverse seismic reduction and isolation of the bridge based on the structural performance-oriented method. New types of dynamic control devices, EVFDs and CSFABs, are adopted in this bridge to analyze the seismic reduction effect. The response difference caused by site categories is also studied. And the optimal design for the parameters of the EVFDs is conducted according to different site categories.

2 Project and Modeling

An asymmetric single-tower double-deck cable-stayed bridge with a steel truss beam is established. The span arrangement is (90+128) m, and the force-resistant style is a semi-floating system with a double cable plane. The upper deck and the lower deck are both one-way three-lane designs. The truss beam is triangular, with the truss panel length of 12 m in the 128 m-span and 9 m in the 90 m-span. The truss height is 9 m, and the transverse distance is 14.55 m.

The tower is in the shape of a pagoda from the cross and a single column from the longitudinal. A cross-beam in the middle of the tower supports the truss beam by the spherical steel bearings. The tower is connected with the cap, and there are 18 bored piles with a diameter of 1.8 m under the cap. There are 18 pairs of spatial cables in a fan-shaped arrangement. The distance between anchorages on the 90 m-span beam is 9 m and the 128 m-span beam is 12 m. The distance between anchorages on the tower is 2 m.

This bridge is a semi-floating system. The truss beam can longitudinally slide on 1♯ pier, 2♯ tower, and 3♯ pier. Among all the spherical steel bearings, the left bearings are laterally fixed, and the right bearings are lateral sliding. There are four lateral wind-resistant bearings between the truss beam and tower. Fig.5 shows the general layout elevation of the bridge. Fig.6 shows the original support scheme of the bridge.

MIDAS Civil is used to construct the dynamic model of the bridge. The X-direction is the longitudinal direction of the bridge, and the Y-direction is
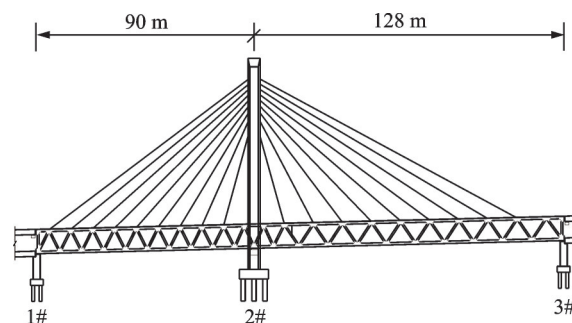
Fig.5 General layout elevation for the (90+128) m cable-stayed bridge
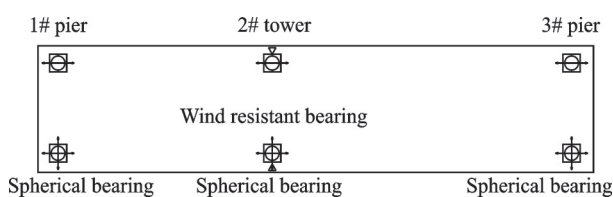
Fig.6 Original support scheme for the (90+128) m cable-stayed bridge

the transverse direction of the bridge. The middle tower, the side piers, the cap, and the pile foundation are all made of concrete and simulated by beam elements. The truss beam is made of steel and simulated by beam element, and the cable is simulated by the truss element. The modeling length of the pile foundation is 10 times the pile diameter to simulate pile-soil interaction. The effect of initial stress is considered, and the Ernst formula is used to modify the elastic modulus. The spatial finite element model is shown in Fig.7.
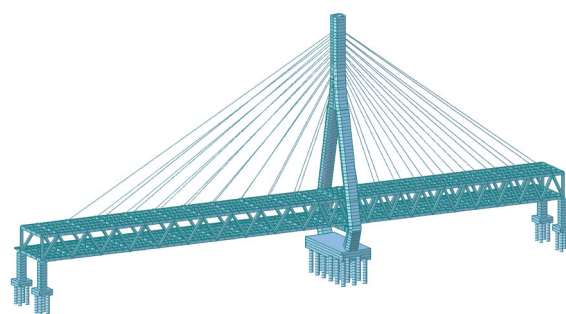
Fig.7 Spatial finite element model by MIDAS Civil

According to the current Code for Seismic Design of Highway Bridge in China (JTG/T 2231-01—2020)[17], this bridge belongs to class B. The return period of E2 earthquake action is 2 000 years, and the importance coefficient $C_i =$ 1.7. Assuming that the bridge site is divided into the second group (unadjusted characteristic period

$T_g = 0.40$ s), Table 1 shows characteristic period T_g, peak acceleration S_{max}, and A of the E2-level design acceleration response spectrum of different site categories [Ⅰ₀, Ⅱ, Ⅳ] in fortification intensity Ⅸ (0.40 g) degree. Fig.8 shows the E2-level design acceleration response spectrum. Fig.9 shows the E2-level seismic acceleration time history waves of different site categories [Ⅰ₀, Ⅱ, Ⅳ].

Table 1　E2-level design acceleration response spectrum parameter table (Fortification intensity IX (0.40 g) degree)

Site Ⅰ 0			Site Ⅱ			Site Ⅳ		
T_g/s	S_{max}/(m·s⁻²)	A/(m·s⁻²)	T_g/s	S_{max}/(m·s⁻²)	A/(m·s⁻²)	T_g/s	S_{max}/(m·s⁻²)	A/(m·s⁻²)
0.25	15.00	3.92	0.4	16.67	3.92	0.75	15.00	3.92
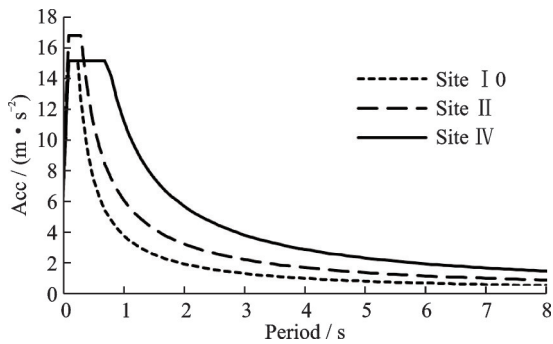
Fig.8　Design acceleration response spectrum

According to the data, site category has a little impact on peak acceleration S_{max} and a significant impact on characteristic period T_g in high intensity Ⅸ degree area. The influence of site category on acceleration response spectrum is mainly reflected in the platform length of the curve. The worse the site category, the longer the platform improves the seismic response.

(a) Site Ⅰ 0　　　(b) Site Ⅱ　　　(c) Site Ⅳ
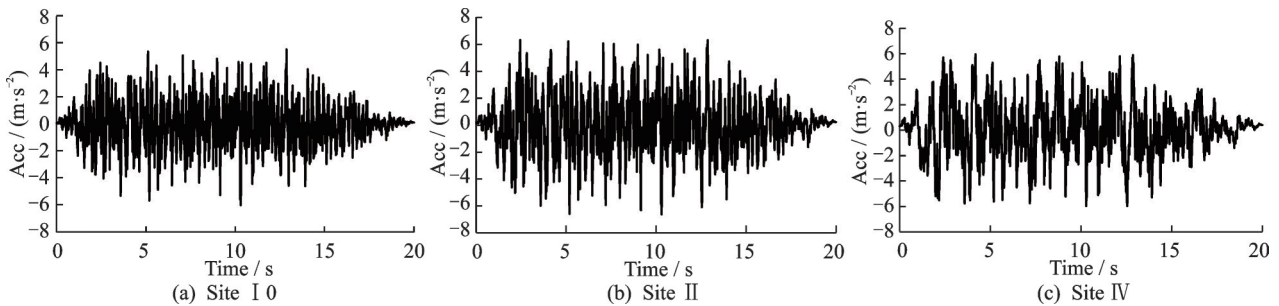
Fig.9　Seismic acceleration time history waves

3　Seismic Reduction and Isolation Schemes

Table 2 shows the three support schemes to contrast the seismic reduction. Among those schemes, Scheme One is the original design as a reference without dynamic control device, as shown in Fig.6.

Table 2　Design table of support schemes

Scheme	Device arrangement	Figure
One (Original)	1♯, 2♯ and 3♯ with spherical bearings 2♯ with lateral wind resistant bearings Without dampers between towers and the beam	Fig.6
Two (Recommended)	1♯ and 3♯ with CSFABs, 3♯ with spherical bearings 2♯ with lateral wind resistant bearings With EVFDs between towers and the beam	Fig.10
Three (Contrastive)	1♯, 2♯ and 3♯ with friction pendulum bearings(FPBs) Without lateral wind resistant bearings between towers and the beam Without dampers between towers and the beam	Fig.11

Scheme Two is the recommended seismic reduction design with new types of device-CSFABs and EVFDs, as shown in Fig.10. It should be noted that the cable of CSFABs is set to work under transvese earthquakes and not work under longitudinal earthquakes to ensure the EVFDs work normally. Scheme Three is the contrastive seismic reduction and isolation design with friction pendulum bearings (FPBs), as shown in Fig.11. FPBs are a kind of friction energy dissipation isolation bearings with excellent performance[18-20]. They make the superstructure swing through the movement of the spherical sliding surface of the bearings. While swinging, the natural vibration period of the bridge structure will be controlled by the spherical curvature radius, and the FPBs also help the bridge to reset after earthquakes.
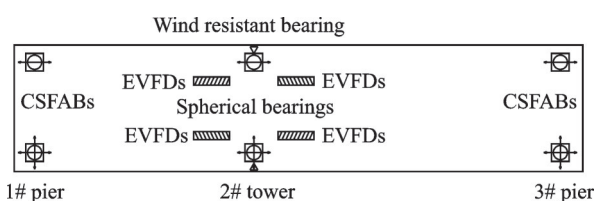
Fig.10 Arrangement of dynamic control devices for Scheme Two
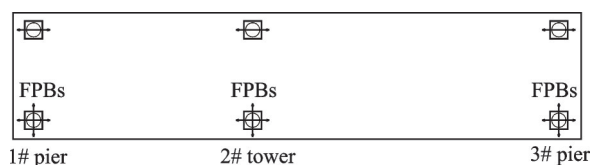
Fig.11 Arrangement of dynamic control devices for Scheme Three

4 Dynamic Characteristics for the Bridge

Table 3 shows the first four vibration frequencies, and Figs.12—15 show the first four vibration

Table 3 The first four steps of the vibration mode frequency and period in the case of Scheme One

Step	Period/s	Vibration mode
1	6.21	Longitudinal drift of the whole beam
2	2.30	Transverse bending of the 128 m-span beam
3	1.80	Transverse bending of the 90 m-span beam
4	1.10	Transverse bending of the 128 m-span beam
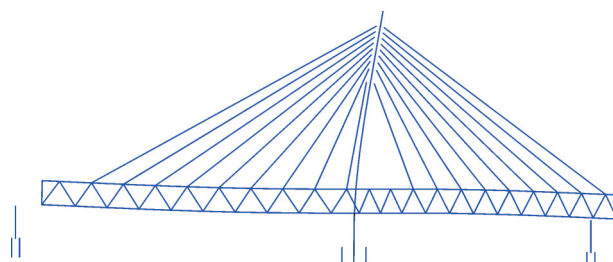
Fig.12 The first step of vibration mode(T_1=6.21 s)

Fig.13 The second step of vibration mode(T_2=2.30 s)

Fig.14 The third step of vibration mode(T_3=1.80 s)
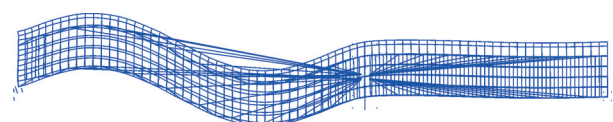
Fig.15 The fourth step of vibration mode(T_4=1.10 s)

modes of this bridge in the case of Scheme One.

According to the analysis of dynamic characteristics, the longitudinal vibration mode period of the bridge is longer, and the transverse vibration mode period is shorter, mainly due to the structural system of longitudinal release and transverse fixed. In addition, due to the large transverse stiffness of the steel truss beam, the transverse vibration mode period of the bridge is shorter than that of a conventional single-deck cable-stayed bridge, which is close to a practical continuous beam bridge. According to the response law, the emergence of transverse short-period vibration mode will cause greater force response, while the longitudinal long-period vibration mode will cause greater displacement response.

Table 4 and Fig.16 show the change of the first-step longitudinal vibration mode and period by the elastic stiffness of spring (K, kN/m) with the damping parameters constant (the damping coefficient C=4 000 kN·s·m^{-1}, the velocity index α=0.3) in case of Scheme Two. Since the dampers have a much lower effect on the static behaviors, it can be inferred that the vibration mode has a mini-

Table 4 The first-step longitudinal vibration mode and period in the case of Scheme Two

$K/(\mathrm{kN \cdot m^{-1}})$	Period/s	Vibration mode	$K/(\mathrm{kN \cdot m^{-1}})$	Period/s	Vibration mode
3 000	4.72		10 000	3.38	
25 000	2.41		50 000	1.86	
100 000	1.47		250 000	1.24	
500 000	1.18		1 000 000	1.16	
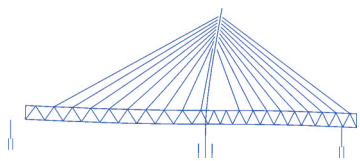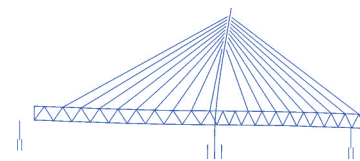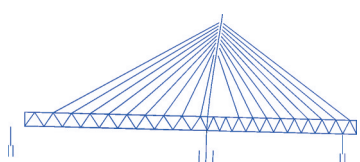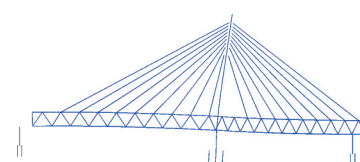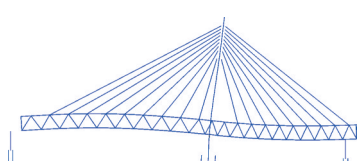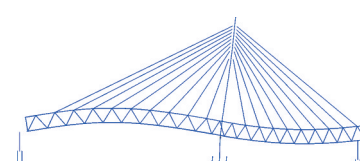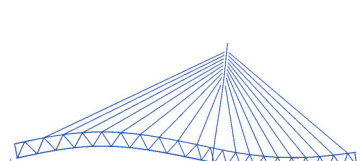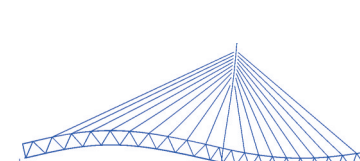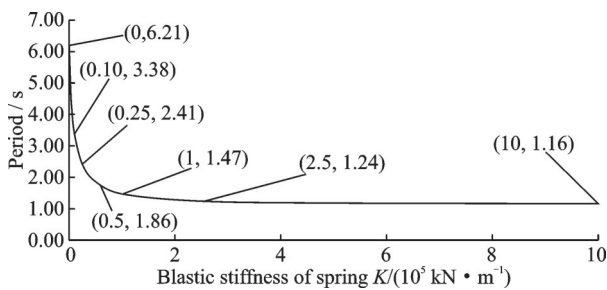
Fig.16 The first-step longitudinal vibration period in the case of Scheme Two

mal correlation with C and α. It can be inferred that the longitudinal vibration mode and period are significantly affected by the elastic stiffness of the spring (K, kN/m). The first-step longitudinal vibration period decreases with K increasing. The structure gradually turns from floating to fixed with K increasing. When K ranges from 0 to 50 000 kN/m, the first-step longitudinal vibration period decreases rapidly from 6.21 s to 1.86 s. When K ranges from 50 000 kN/m to 250 000 kN/m, the first-step longi-

tudinal vibration period decreases slowly from 1.86 s to 1.24 s. When K ranges from 250 000 kN/m to 1 000 000 kN/m, the first-step longitudinal vibration period tends to be stable at 1.20 s, and the structure is an almost fixed pylon-beam system. According to the response law, it can be inferred that the seismic displacement of the beam decreases with K increasing. However, the change law for the internal seismic force needs further study to discuss.

Fig.17 shows the variable period and the E2-level design acceleration response spectrum of different site categories in the same fortification intensity Ⅸ (0.40 g) degree. According to the curve trend, the first-step longitudinal vibration period of 2 s is suggested, such as K equal to 50 000 kN/m, to satisfy the seismic requirements and prevent the performance surplus. There are some differences between the spectrum curves of different site categories, which may effect the best choice for K. However, it
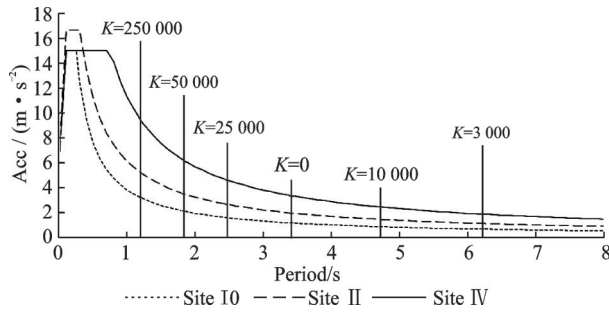
Fig.17　Influences of the elastic stiffness K on the first-step longitudinal period of the structure

Fig.18　Contrast of beam-end displacement at 1# pier with longitudinal seismic

Fig.19　Contrast of tower bottom bending moment with longitudinal seismic

is only a qualitative judgment for the choice of K by the period curve. But the accurate judgment should depend on the further calculation.

5　Research for Longitudinal Seismic Reduction System

The main problem for the longitudinal seismic reduction and isolation design of double-deck cable-stayed bridges in high intensity(Ⅸ degree) areas is the excessive beam displacement and tower bottom bending moment. EVFDs and FPBs are two kinds of seismic isolation devices to solve these problems. A contrast of the longitudinal seismic-reduction effect among the three schemes mentioned before has been conducted by nonlinear time history analysis with the E2-level seismic acceleration time history waves of different site categories in the same fortification intensity Ⅸ (0.40 g) degree.

5. 1　Parameters of seismic reduction devices

Scheme One：Without dynamic control devices.

Scheme Two：the damping coefficient C is set as 4 000 kN·s·m^{-1}, the velocity index α is 0.3, and the elastic stiffness of spring K is 50 000 kN/m.

Scheme Three：The radius of curvature of FPBs is set as 4 m. The sliding friction coefficient of bearings is 0.02, and the relative displacement before sliding is 2 mm.

5. 2　Contrast of longitudinal seismic response reduction

Figs.18,19 show the contrasts of the beam-end displacement and the tower bottom bending moment among the three schemes. According to the comparison results of longitudinal beam-end displacement, the reduction effect of FPBs is far less than that of EVFDs, especially in the case of site categories Ⅱ and Ⅳ. This is related to the working characteristics of EVFDs. With the increase in speed, the damping force increases exponentially and effectively consumes seismic energy. Comparing the beam-end displacement reduction rate, the FPBs scheme can achieve an ideal reduction rate in site category Ⅰ0, close to 60%. However, the rate decreases significantly in site categories Ⅱ and Ⅳ. The beam-end displacement reduction rate of the EVFDs scheme does not change significantly with the site category, and the rate remains at about 75%.
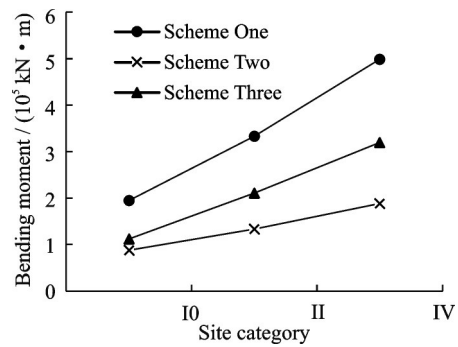
The comparison results of the longitudinal seismic bending moment at tower bottom show that the tower bottom bending moment reduction of the EVFDs scheme is better than that of the FPBs scheme. Comparing the seismic reduction rate listed in Tables 5, 6, the FPBs scheme can achieve nearly 40%. In comparison, the EVFDs scheme has a significant seismic reduction effect with reduction rate nearly 60%.

Table 5   Contrast of beam-end displacement at 1# pier with longitudinal seismic

Site category	Beam-end displacement/m			Reduction rate/%	
	Scheme One (Original)	Scheme Two (Recommended)	Scheme Three (Contrastive)	Scheme Two (Recommended)	Scheme Three (Contrastive)
I 0	0.602	0.130	0.242	78	60
II	1.083	0.273	0.535	75	51
IV	1.874	0.490	1.044	74	44

Table 6   Contrast of tower bottom bending moment with longitudinal seismic

Site category	Bending moment/(kN·m)			Reduction rate/%	
	Scheme One (Original)	Scheme Two (Recommended)	Scheme Three (Contrastive)	Scheme Two (Recommended)	Scheme Three (Contrastive)
I 0	194 954	87 728	111 942	55	43
II	332 937	133 658	210 744	60	37
IV	498 605	188 190	319 254	62	36

5.3   Parameter optimization design for EVFDs

Assuming the velocity index $\alpha=0.3$, research to discuss the relationship between seismic responses and device parameters (damping coefficient C and elastic stiffness K)is conducted[21-23]. Fig.20 shows the beam-end displacement at 1# pier and Fig.21 shows the tower bot-

(a) In case of C=1 000 kN·s·m^{-1}

(b) In case of C=3 000 kN·s·m^{-1}

(c) In case of C=5 000 kN·s·m^{-1}
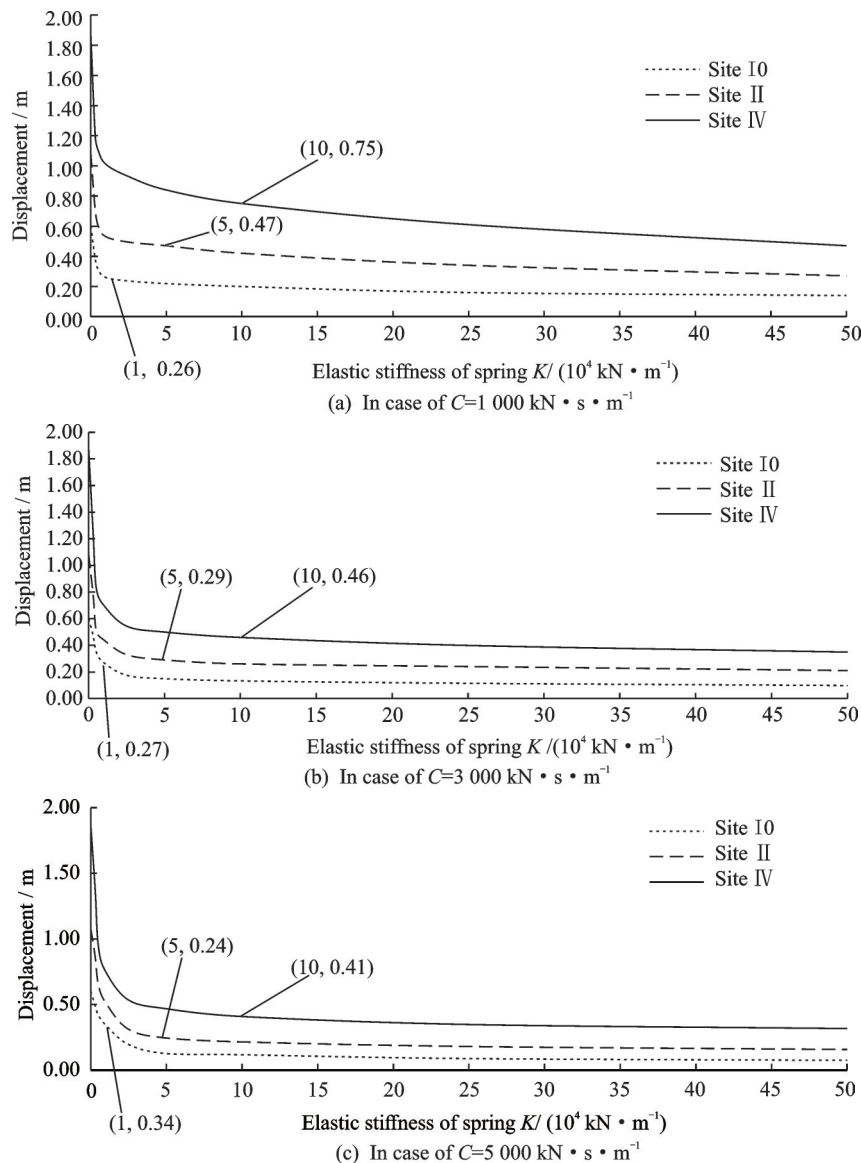
Fig.20   Influences of the elastic stiffness of spring K on the beam-end displacement at 1# pier under longitudinal seismic
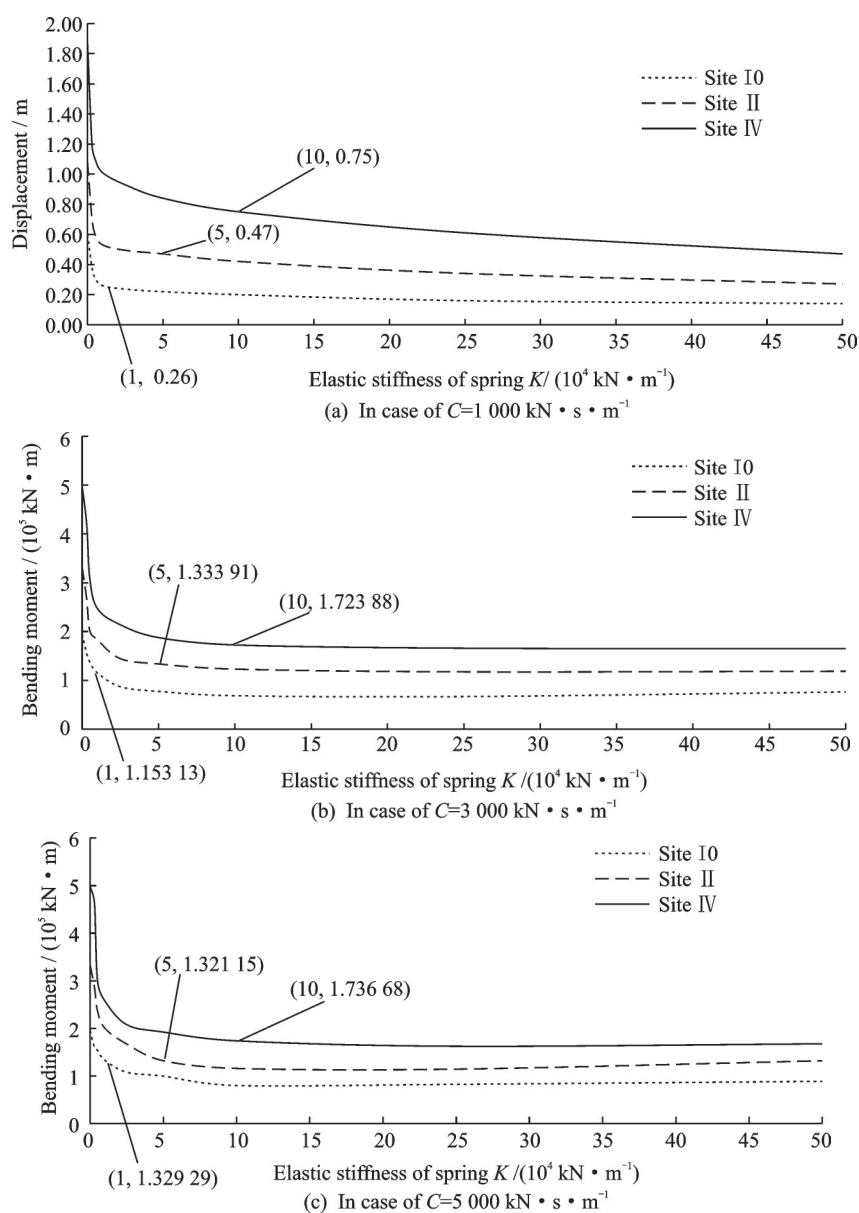
Fig.21   Influences of the elastic stiffness of spring K on the tower bottom bending moment under longitudinal seismic

tom bending moment with different K and C.

It can be inferred that the elastic stiffness of spring K of EVFDs has a dramatic effect on both seismic displacement and internal force. The seismic responses decrease rapidly with K increasing in the range of K from 0 to 25 000 kN/m. In the range of K from 25 000 kN/m to 100 000 kN/m, the seismic responses decrease slowly with K increasing. In the range of K from 100 000 kN/m to 500 000 kN/m, the seismic responses remain stable in case of sites Ⅱ and Ⅳ but decrease very slowly of site Ⅰ0. To keep the beam-end displacement under 0.3 m in case of sites Ⅰ0 and Ⅱ, the K is suggested to be set as 10 000 kN/m in site Ⅰ0 and 50 000 kN/m in

site Ⅱ. To keep the beam-end displacement under 0.4 m in case of site Ⅳ, the K is suggested to be set as 100 000 kN/m.

Based on the above suggested elastic stiffness of spring K of EVFDs, the influences of the damping coefficient C on longitudinal seismic responses are conducted, as shown in Figs.22—24.

It can be inferred that the damping coefficient C of EVFDs has a significant effect in case of sites Ⅱ and Ⅳ and a relatively insignificant impact in case of site Ⅰ0. The C is suggested to be set as 2 000 kN·s·m^{-1} in site Ⅰ0, 4 000 kN·s·m^{-1} in site Ⅱ and 6 000 kN·s·m^{-1} in site Ⅳ. Table 7 shows the recommended values of the design parameters.
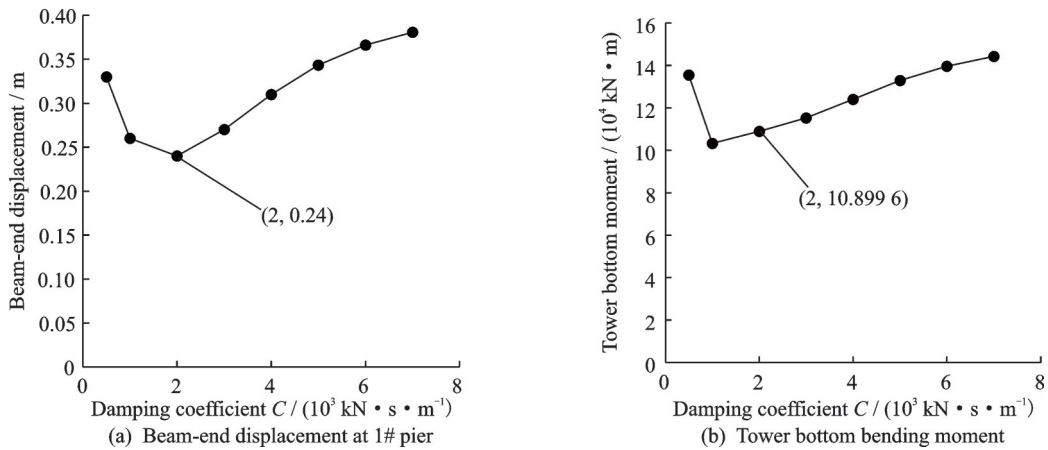
Fig.22   Influences of damping coefficient C on longitudinal seismic response of site category Ⅰ₀ (in case of $K=10\ 000$ kN/m)
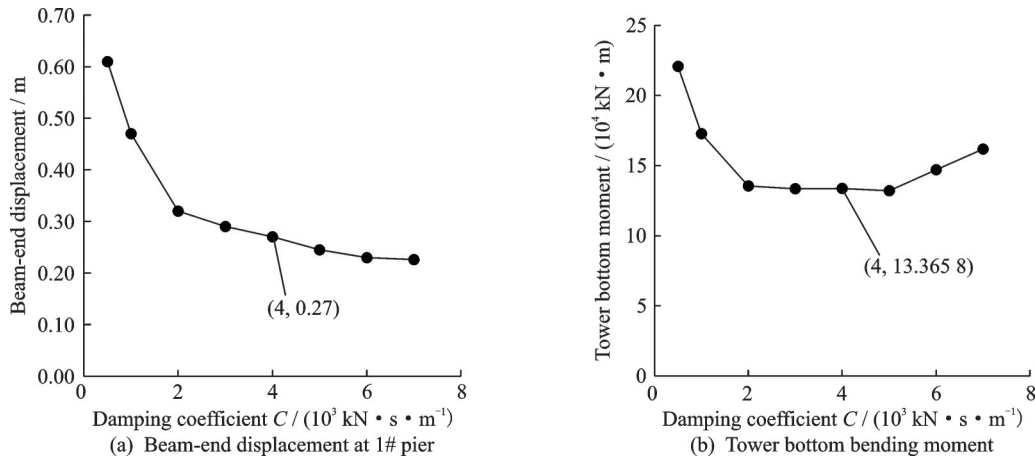
Fig.23   Influences of damping coefficient C on longitudinal seismic response of site category Ⅱ (in case of $K=50\ 000$ kN/m)
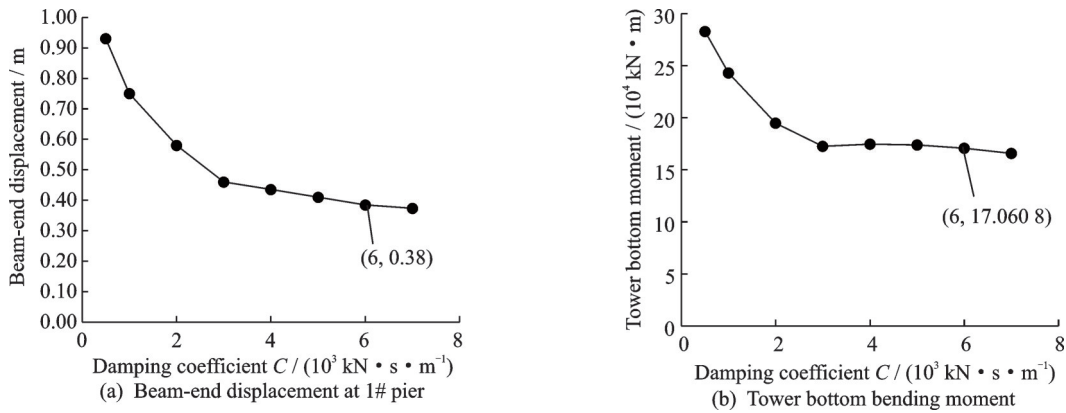
Fig.24   Influences of damping coefficient C on longitudinal seismic response of site category Ⅳ (in case of $K=100\ 000$ kN/m)

Table 7   Recommended values of parameters for EVFDs (fortification intensity Ⅸ (0.40 g) degree)

Site category	Damping coefficient C / (10^3 kN·s·m^{-1})	Elastic stiffness of spring K / (10^4 kN·m^{-1})
Ⅰ₀	2	1
Ⅱ	4	5
Ⅳ	6	10

6   Research on Transverse Seismic Reduction System

The main problem for the transverse seismic reduction and isolation design of double-deck cable-stayed bridges in high intensity (Ⅸ degree) areas is that the excessive bearing shear force on the side pier may lead to the lateral shear of the bearing and

risk of the beam falling. Double-deck bridges have a higher risk of lateral sliding with beam-dropping than single-deck bridges because of the high truss, which maybe causes unforeseeable damages. The conventional method of using a stopper to prevent beam falling cannot balance the displacement of the superstructure and the internal force of the substructure. In case of improper design, the side pier may be damaged due to an over robust stopper design.

CSFABs and FPBs are two kinds of dynamic control devices to release the displacement of the superstructure and reduce the internal force of the substructure. However, they have different working principles and appropriate situations. A contrast of the transverse seismic-reduction effect among the three schemes mentioned before has been conducted by nonlinear time history analysis with the E2-level seismic acceleration time history waves of different site categories in the same fortification intensity Ⅸ (0.40 g) degree.

6. 1 Parameters of seismic reduction devices

Scheme One: Without dynamic control devices.

Scheme Two: The horizontal stiffness of the cable is set as 600 000 kN/m. The free-displacement u_0 of CSFABs is set as 0.2 m. The sliding friction coefficient of bearings is 0.02, and the relative displacement before sliding is 2mm.

Scheme Three: The radius of curvature of FPBs is set as 4 m. The sliding friction coefficient of bearings is 0.02, and the relative displacement before sliding is 2 mm.

6. 2 Contrast of transverse seismic response reduction

The transverse nonlinear seismic time history analysis is conducted to contrast the beam-end displacement, the tower bottom bending moment, and the side pier bottom bending moment among the three schemes, as shown in Figs.25—27 and Tables 8,9.

Comparing the analysis results of beam-end displacement, we find there is a large lateral beam-end displacement of more than 0.5 m with FPBs adopt-
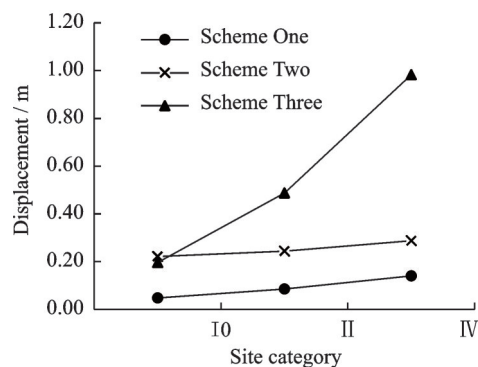
Fig.25　Contrast of beam-end displacement at 1♯ pier under transverse seismic
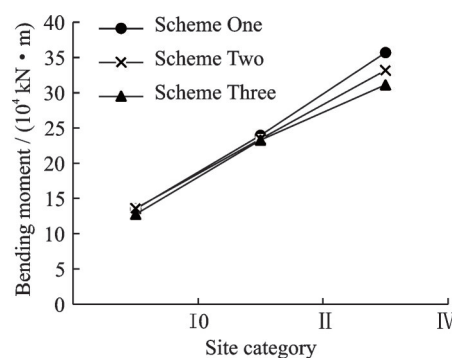
Fig.26　Contrast of tower bottom bending moment
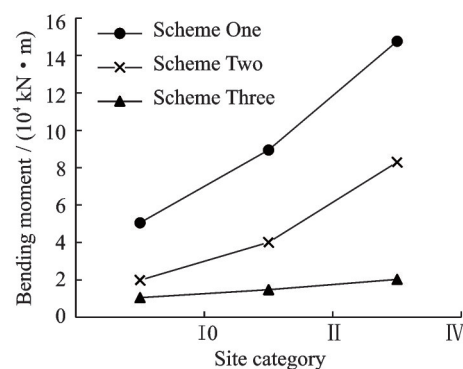
Fig.27　Contrast of 1♯ pier bottom bending moment

ed in the case of site categories Ⅱ and Ⅳ, which does not meet the design requirements and has a high risk of beam falling. On the contrary, CSFABs can effectively control the relative displacement of pier and beam in the range of less than 0.3 m, which is more reasonable. Comparing the analysis results of pier bottom bending moment, we find the reduction of pier internal force by CSFABs is less than that by FPBs, but it can still reach 45%—60%. Besides, the reduction of tower bottom bending moment is not obvious.

Table 8   Contrast of beam-end displacement at 1# pier with transverse seismic

Site category	Beam-end displacement/m			Increasing rate/%	
	Scheme One (Original)	Scheme Two (Recommended)	Scheme Three (Contrastive)	Scheme Two (Recommended)	Scheme Three (Contrastive)
I 0	0.048	0.221	0.197	362	310
II	0.085	0.244	0.488	186	472
IV	0.140	0.288	0.983	105	600

Table 9   Contrast of bending moment at 1# pier bottom with transverse seismic

Site category	Bending moment/(kN•m)			Reduction rate/%	
	Scheme One (Original)	Scheme Two (Recommended)	Scheme Three (Contrastive)	Scheme Two (Recommended)	Scheme Three (Contrastive)
I 0	50 468	19 771	10 429	61	79
II	89 546	40 088	14 714	55	84
IV	147 624	82 926	20 186	44	86

7   Conclusions

Taking a double-deck cable-stayed bridge with a truss beam as the research object, we analyze the longitudinal and transverse seismic response law for this bridge of different site categories in fortification intensity IX (0.40 g) degree area to contrast the seismic reduction between new types of dynamic control devices (EVFDs and CSFABs) and conventional devices (FPBs). A seismic-reduction support system is designed for double-deck cable-stayed bridges with truss beams to reduce seismic responses and ensure the expansion joints and bearings are normally working. The influences of the damping coefficient C and the elastic stiffness of spring K of EVFDs are studied, and the parameter optimization design is conducted. The following conclusions and practical suggestions are drawn from the research.

（1）With the conventional longitudinal release and lateral restraint system adopted, the longitudinal vibration mode period of the bridge is long and the transverse vibration mode period is short. The beam displacement is the main factor that should be considered in the longitudinal seismic design. Moreover, the bearing shear as well as side pier internal force are the main factors that should be considered in the transverse seismic design.

（2）With the contrast between the new seismic-reduction supported system and the conventional FPBs supported system, it can be inferred that the new seismic-reduction supported system composed of EVFDs and CSFABs plays a better function under both seismic and normal work to prevent the expansion joints damage. It can reduce the beam-end displacement by 75% and the tower-bottom bending moment by 60% under longitudinal seismic. Besides, it can reduce the pier-bottom bending moment by at least 45% under transverse seismic as well as control the relative displacement between pier and beam under 0.3 m. It is a sustainable seismic-reduction system for the double-deck cable-stayed bridge with a truss beam.

（3）Results show that the first-step longitudinal vibration period decreases with the elastic stiffness of spring K of EVFDs increasing. The structure gradually turns from floating to fixed with K increasing. When K ranges from 0 to 50 000 kN/m, the first-step longitudinal vibration period decreases rapidly. When K ranges from 50 000 kN/m to 250 000 kN/m, the first-step longitudinal vibration period decreases slowly. When K ranges from 250 000 kN/m to 1 000 000 kN/m, the first-step longitudinal vibration period tends to be stable, and the structure is almost a fixed pylon-beam system.

（4）Assuming the velocity index $\alpha = 0.3$, the relationship between longitudinal seismic responses and EVFDs parameters shows that the elastic stiffness of spring K of EVFDs dramatically affects both seismic displacement and the internal force in case of all site categories. In contrast, the damping coeffi-

cient C of EVFDs has a significant effect in the case of sites Ⅱ and Ⅳ and a relatively insignificant impact in the case of site Ⅰ0. The parameter optimization suggests C is set as 2 000 kN·s·m^{-1} in site Ⅰ0, 4 000 kN·s·m^{-1} in site Ⅱ, 6 000 kN·s·m^{-1} in site Ⅳ, and K is set as 10 000 kN/m in site Ⅰ0, 50 000 kN/m in site Ⅱ, and 100 000 kN/m in site Ⅳ.

References

[1] SUN Jianyuan, CHEN Jieliang. Conceptual design of double-deck traffic for city bridge[J]. Bridge Construction, 2006(2): 39-42. (in Chinese)

[2] YE Aijun. Seismic design of bridge[M]. Beijing: The People's Communication Publishing Company, 2017: 121-125. (in Chinese)

[3] GUAN Zhongguo, LI Jianzhong. Advances in earthquake resisting systems for long-span bridges[J]. Scientia Sinica Technologica, 2021, 51(5): 493-504. (in Chinese)

[4] JAMI M, RUPAKHETY R, ELIAS S, et al. Recent advancement in assessment and control of structures under multi-hazard[J]. Applied Sciences, 2022, 12 (10): 5118.

[5] XIAO Kaiqian, XU Huaibing, LIU Min, et al. Seismic performance analysis and vibration control study of one cable-stayed bridge[J]. Journal of Natural Disasters, 2020, 29(1): 57-63. (in Chinese)

[6] YI J, ZHOU J Y, YE X J. Seismic control of cable-stayed bridge using negative stiffness device and fluid viscous damper under near-field ground motions[J]. Journal of Earthquake Engineering, 2022, 26(5): 2642-2659.

[7] LIU X L, HUANG Q, REN Y. Analysis on deflection characteristics of steel cable-stayed bridge[J]. Transactions of Nanjing University of Aeronautics and Astronautics, 2018, 35(5): 890-895.

[8] FENG P C, SUN Y, FU K, et al. Application study of new elasticity-damping composite device on Zhuankou Yangtze river highway bridge[J]. Journal of Bridge Engineering, 2019, 24(1): 1-23.

[9] JIAO Changke. Research on seismic response and its vibration control of double-deck long-span cable-stayed bridge[D]. Nanjing: Southeast University, 2012. (in Chinese)

[10] XING Liang. Modal analysis and seismic response of the steel truss cable-stayed bridge with double deck[J]. Highway, 2021, 66(1): 130-136. (in Chinese)

[11] ZHANG Yu. Seismic response analysis of different structrual systems of steel truss cable-stayed bridges[D]. Wuhan: Wuhan University of Technology, 2013. (in Chinese)

[12] DANG Xinzhi, YUAN Wancheng, PANG Yutao, et al. Development and application of the self-centering cable-sliding friction aseismic device[J]. Journal of Harbin Engineering University, 2013, 34(12): 1537-1543. (in Chinese)

[13] YUAN Wancheng, WEI Zhenghua, CAO Xinjian, et al. Cable-sliding friction aseismic bearing and its application in bridge seismic design[J]. Engineering Mechanics, 2011, 28(S2): 204-209. (in Chinese)

[14] LI R, YUAN X, YUAN W, et al. Seismic analysis of half-through steel truss arch bridge considering superstructure[J]. Structural Engineering and Mechanics, 2016, 59(3): 387-401.

[15] YANG H, PANG Y, TIAN S, et al. Case study of the seismic response of an extra-dosed cable-stayed bridge with cable-sliding friction aseismic bearing using shake table tests[J]. The Structural Design of Tall and Special Buildings, 2017, 26(16): 1398.

[16] GUO J, ZHONG J, DANG X, et al. Seismic performance assessment of a curved bridge equipped with a new type spring restrainer[J]. Engineering Structures, 2017, 151: 105-114.

[17] Ministry of Transport of the People's Republic of China. Code for seismic design of highway bridges in China: JTG/T 2231-01—2020 [S]. Beijng, China: [s. n.], 2020.

[18] YU Z, LI H, WEI B, et al. Numerical analysis on longitudinal seismic responses of high-speed railway bridges isolated by friction pendulum bearings[J]. Journal of Vibroengineering, 2018, 20(4): 1748-1760.

[19] GAO Jun, LIN Xiao. Analysis of damping performance of frictional pendulum bearings in long-span cable-stayed bridge[J]. Bridge Construction, 2020, 50 (2): 55-60. (in Chinese)

[20] CHEN Y, SUN H, FENG Z. Study on seismic isolation of long span double deck steel truss continuous girder bridge[J]. Applied Sciences, 2022, 12(5):2567.

[21] ZHONG J, NI M, HU H, et al. Uncoupled multivariate power models for estimation performance-based seismic damage states of column curvature ductility[J]. Structures, 2022, 36: 752-764.

[22] HE X, YANG Y, XIAO X, et al. Research on fluid viscous damper parameters of cable-stayed bridge in northwest China[J]. Shock and Vibration, 2017(6): 1-9.

[23] SHI Jun，XU Lueqin，ZHOU Jianting，et al. Parameter optimization analysis of viscous dampers for cable-stayed bridges with floating system based on response surface method[J]. Earthquake Resistant Engineering and Retrofitting，2022,44(1)：80-87. (in Chinese)

Author Dr. CHEN Suhua graduated from Southeast University with a master's degree in Road and Railway Engineering in 1999 and recieved her Ph.D. degree from Southeast University in 2011. She joined Architects & Engineers Co. Ltd. of Southeast University in 1999 and served as deputy chief engineer of the transport branch from 2008 and road and bridge major chief engineer from 2020.

新型动力控制装置的受力分析和数值模拟

陈素华[1,2]，李瑞琪[2]，费　梁[2]，于智光[2]，丁健明[1,2]

（1.东南大学交通学院，南京 210096，中国；2.东南大学建筑设计研究院有限公司，南京 210096，中国）

摘要：由于耐久性不足,常规黏滞阻尼器等动力控制装置不适用于双层钢桁梁斜拉桥减隔震设计。本文提出高性能的新型动力控制装置应用于双层钢桁梁斜拉桥抗震设计的研究思路,基于一座抗震设防烈度Ⅸ度区的跨径（90＋128）m 的双层钢桁梁斜拉桥,建立三维有限元分析模型,进行地震动时程分析,应用两种新型动力控制装置-弹性索组合黏滞阻尼器以及拉索减隔震支座,进行地震作用下的结构受力分析及数值模拟,针对弹性索组合黏滞阻尼器的设计参数-弹性索水平刚度 K 及阻尼系数 C 进行优化设计。研究得出以下结论:(1)由弹性索组合黏滞阻尼器和拉索减隔震支座组合而成的动力控制系统既满足正常使用状态下的耐久性要求,又可以有效减少结构在地震作用下的动力响应。(2)纵向地震动作用下,组合动力控制系统对梁端位移减震率达 75％,塔底弯矩减震率达 60％;横向地震动作用下,组合动力控制系统对边墩底弯矩减震率达 45％,同时可控制墩梁相对位移在 0.3 m 以内。(3)假定阻尼指数 $\alpha＝0.3$,参数优化设计表明,针对场地类别Ⅰ0地区,阻尼系数 C 推荐值为 2 000 kN·s·m^{-1},弹性索水平刚度 K 推荐值为 10 000 kN/m;针对场地类别Ⅱ地区, C 推荐值为 4 000 kN·s·m^{-1}, K 推荐值为 50 000 kN/m;针对场地类别Ⅳ地区, C 推荐值为 6 000 kN·s·m^{-1}, K 推荐值为 100 000 kN/m。

关键词：动力控制装置;双层钢桁梁斜拉桥;拉索减隔震支座;弹性索组合黏滞阻尼器